



**SCIENTIFIC OASIS**

## Decision Making: Applications in Management and Engineering

Journal homepage: [www.dmame-journal.org](http://www.dmame-journal.org)  
ISSN: 2560-6018, eISSN: 2620-0104



# Optimizing High-Speed Train Timetabling with Consideration of Station Carrying Capacity

Chunxiao Chen<sup>1\*</sup>, Wenjing Li<sup>2</sup>

- <sup>1</sup> School of Rail Transit transportation, Hunan Railway Professional Technology College, Zhuzhou 412001, China  
<sup>2</sup> School of Traffic and Transportation Engineering, Central South University, Changsha 410075, China

### ARTICLE INFO

#### Article history:

Received 19 July 2024  
Received in revised form 10 November 2024  
Accepted 9 December 2024  
Available online 10 February 2025

#### Keywords:

High-Speed Railway, Train Timetabling, Carrying Capacity, Genetic Algorithm

### ABSTRACT

The extensive development of high-speed railways (HSR) in China has transformed the railway system from one constrained by limited capacity to a more adaptable network, significantly mitigating previous capacity shortages. Nevertheless, the demand for high-speed rail services exhibits considerable variability, with peak travel periods—such as the Spring Festival, summer holidays, and extended weekends—increasingly becoming regular occurrences. During these peak times, passenger flows become highly concentrated, resulting in temporary congestion at certain high-traffic HSR stations. Current methodologies for assessing the carrying capacity of HSR stations predominantly rely on approaches originally designed for conventional railways. These methods often fail to adequately consider the unique characteristics of individual stations, their equipment, and operational specifics. The parameters employed are frequently broad and lack precision, underscoring the necessity for more refined techniques to calculate station capacity and develop accurate HSR timetables that can better accommodate peak travel demands. This research initially integrates the train dispatching principles of HSR station CTC (Centralised Traffic Control) systems with automatic point sampling principles to conduct a comprehensive analysis of critical parameters. These parameters include train occupancy durations on arrival and departure tracks, train occupancy times in throat areas, and daily idle periods. The values of these parameters are refined and standardised to ensure that the outcomes of the comprehensive analysis method align more closely with actual operational requirements. Subsequently, with the objective of minimising total travel time, this study formulates a single-objective mathematical programming model for generating HSR timetables that incorporate station carrying capacity constraints. A genetic algorithm is also developed to solve this model. Utilising operational data from the Shanghai-Hangzhou East HSR, the study constructs a timetable under the constraints of station capacity, assesses the influence of both the timetable and the algorithm on the results, and verifies the efficacy of the proposed model and algorithm.

\* Corresponding author

E-mail address: [cchunx@126.com](mailto:cchunx@126.com)

<https://doi.org/10.31181/dmame8120251317>

## 1. Introduction

In recent years, the significant increase in the speed and density of high-speed trains, coupled with the growing complexity of operational scenarios, has led to substantial improvements in the

transportation efficiency of China's high-speed rail (HSR) network. Several critical performance indicators have reached or even exceeded global benchmarks, advancing the pursuit of high-quality development in railway transportation. By the end of 2024, China's total railway operating mileage had reached 162,000 kilometres, with HSR operating mileage accounting for 48,000 kilometres—over 70% of the global total and ranking first worldwide. This represents an increase of 37,000 kilometres compared to 2013. HSR has effectively reduced spatial and temporal distances between regions and urban-rural areas, driving industrialisation and urbanisation, accelerating industrial restructuring and upgrades, and making significant contributions to economic and social development. Excluding the period from 2020 to 2022, which was heavily impacted by the COVID-19 pandemic, railway passenger volumes have demonstrated steady annual growth, outpacing the expansion of the railway network. In 2024, railway passenger volume reached 4.312 billion, with 3.272 billion trips made on high-speed trains, accounting for 75.9% of total railway passenger volume. Passenger turnover reached 1,579.91 billion passenger-kilometres, with high-speed rail contributing 1,084.549 billion passenger-kilometres.

According to statistical data, the utilisation rate of China's HSR line capacity exceeds 80% in key sections, particularly along busy mainlines such as the Beijing-Shanghai and Beijing-Guangzhou routes. On certain segments, the number of scheduled train timetables has surpassed 150 pairs, resulting in both capacity constraints and high passenger volumes. In response, railway authorities and scholars have been actively researching methods to optimise train timetables to enhance HSR carrying capacity. HSR carrying capacity can be categorised into two main types: railway station carrying capacity (point) and line carrying capacity (line), collectively referred to as the "point-line" capacity of HSRs. Generally, there is an imbalance between the two, with sufficient line capacity but inadequate railway station carrying capacity. This imbalance makes railway station capacity a bottleneck that restricts the overall transportation efficiency of the HSR network.

The carrying capacity of arrival-departure tracks at HSR stations is calculated using the direct computation method, while the capacity of throat areas is assessed using the utilisation rate method. Both methods fall within the scope of comprehensive analysis and are based on traditional definitions used for conventional railways. However, this approach presents certain inconsistencies. When calculating the carrying capacity of conventional railways, the focus is on marshaling yards, district stations, and intermediate stations that handle passenger and freight services. The proportion of various train operations is determined based on the standard operation time of receiving-departure tracks and throat areas, as well as the resulting empty coefficient, which is then used to calculate the carrying capacity [1].

In contrast, HSR stations are fundamentally different in terms of their operational nature. They primarily handle the operations of high-speed Electric Multiple Unit (EMU) trains, and the operational procedures are significantly different, leading to considerable variations in the operation time of receiving and departure tracks and throat areas compared to conventional railways. This results in discrepancies between the parameter values of the train operation diagram and actual field conditions, ambiguous value standards, and weak dynamicity of calculation results, which significantly increases the risk of being unable to allocate feasible station route resources for trains. Consequently, conventional railway carrying capacity calculation methods cannot be entirely applied to determine the carrying capacity of HSR stations. Moreover, the realisation of "operating trains according to the train timetable" is of paramount importance for HSRs. This necessitates that when trains cannot be allocated viable station route resources, the train timetable must be reconfigured to ensure operational feasibility and efficiency.

The primary contributions of this study are outlined as follows:

1. By incorporating train dispatching principles within the CTC system alongside automatic point

sampling, this study examines critical parameters in the comprehensive analysis method, including train occupancy times on arrival and departure tracks, train occupancy times in throat areas, and daily idle time. It refines and standardises these parameter values to enhance the alignment of the comprehensive analysis method with real-world operational demands.

2. A mixed-integer linear programming (MILP) model has been formulated to address high-speed train timetabling while accounting for station capacity constraints. This model optimises train arrival and departure times and determines the routes for arrival-departure tracks at each station.

3. A genetic algorithm (GA) incorporating a novel encoding and crossover operation is developed to address the model's constraints effectively. This approach significantly enhances the computational efficiency of the model.

4. The proposed MILP model and GA are validated through a case study on the Shanghai Hongqiao–Hangzhou East HSR Line, demonstrating their effectiveness and efficiency.

The remainder of this paper is structured as follows: Section 2 reviews the literature on train timetabling and the integrated optimisation of train scheduling and station operations. Section 3 presents the mathematical formulation, outlining the scenario, assumptions, and parameters. Section 4 introduces the proposed GA for solving the model. Section 5 details a numerical case study evaluating the model and algorithm's effectiveness. Finally, Section 6 presents conclusions and future research directions.

## **2. Literature Review**

### *2.1 Train Timetabling*

In 1989, [2] introduced the Periodic Event Scheduling Problem (PESP), which was subsequently applied to train timetabling by [3]. This application marked the inception of research into the periodic train timetable problem. The process of constructing a periodic train timetable begins by establishing a short time (typically one hour), followed by replicating this schedule across other feasible time slots. During peak periods, the timetable is generally designed to operate at full capacity, while off-peak times may involve the suspension of certain services, such as through line reductions. There are two main variants of train timetable: one involves a cyclic (or periodic) schedule, repeated at every given time (e.g., every hour). Periodic timetabling aids passengers in memorising departure times, ensures smoother connections across routes, and simplifies the scheduling problem. Consequently, it has gained widespread adoption by transportation companies abroad, particularly in countries such as Germany and the Netherlands. The primary methods employed in this research include the maximum algebraic method, graph theory-based approaches, metaheuristic algorithms [4], constraint generation algorithms [5], and stochastic optimisation techniques [6]. In general, the optimisation objectives for non-periodic timetables are approached from the perspectives of transportation companies, passengers, or a combination of both [7]. These objectives primarily focus on maximising the operational benefits of the company, maximising the profit functions of all trains, minimising energy consumption in train operations [7, 8], minimising total travel time [9], reducing average passenger waiting time, minimising turnaround times for high-speed trains, and maximising train schedule capacity. The methods used in this research include branch-and-bound algorithms [10-15], Lagrangian relaxation algorithms [11, 16-19], column generation algorithms [20, 21], and heuristic algorithms [22-26].

### *2.2 Integrated Optimization of Train Timetabling and Railway Station Operations Schedule*

Some experts have also explored the integrated optimisation of train timetabling and railway station operation schedules from the perspective of comprehensive optimisation of train operation

schedules, line planning, and station stop planning. Train line planning plays a vital role in linking passenger service demand with railway transportation organisation. In traditional railway planning processes, output data from line planning, such as station stop planning, are typically used as input for optimising the train timetable. However, because train line planning often neglects the specific operation times of trains in sections and stations, discrepancies with real-world conditions may arise. Furthermore, inefficient stop planning can limit capacity and service quality. As a result, some researchers have studied this issue from the standpoint of integrated optimisation of line planning, train timetabling, and stop planning. The authors in [27] conducted extensive research on the integrated optimisation of train operation plans and schedules, proposing a bi-level programming model aimed at maximising the operational efficiency of railway enterprises.

The lower-level model addresses passenger travel behaviour within a transfer network, allowing passengers to choose travel options based on factors such as ticket prices, arrival and departure times, transfer times, and congestion costs. The authors in [28] proposed an integrated optimisation model for train schedules and operation plans, aiming to minimise both enterprise operating costs and passenger time costs, including waiting times at stations, transfer times at interchange stations, and travel times within sections. They employed a cross-entropy algorithm to solve the problem. The authors in [29] examined the collaborative optimisation of stop planning and train timetables under HSR corridor conditions, developing a multi-objective mixed-integer programming model and solving it with GAMS and ILOG CPLEX. The authors in [30] proposed an integrated optimisation model combining high-speed train timetables and stop planning to meet both passenger service demands and train line planning requirements, using Lagrangian relaxation and column generation algorithms to solve the problem. The authors in [31] developed a timetable optimisation model considering a predetermined skip-stop pattern and origin-destination (OD) passenger demand. The authors in [32] presented a method to increase the number of scheduled trains on a line by adjusting train dwell times and stop plans, solving the problem using a Lagrangian-based heuristic algorithm.

### **3. Mathematical Formulation**

#### *3.1 Problem Statement*

China's HSR system employs a collinear operation model for medium and high-speed trains, with train timetabling based on the railway line as the fundamental unit. In this model, a station is represented as a node, while the interval is denoted by the start and end stations of the respective section. The set of stations and intervals together form the railway line set. The train timetable in this study is defined as the optimisation of a timetable that minimises the total travel time of trains across a given set of railway lines and trains. This objective must be achieved without exceeding track capacity and while adhering to operational constraints, such as skylight management and the allocation of arrival-departure tracks. In constructing the model, the traditional interval-based train operation diagram representation is maintained, with the time required for trains to pass through nodes considered as zero.

#### *3.2 Assumptions*

Before detailing the model formulation for high-speed train timetable in this paper, the following assumptions are outlined to simplify the problem under consideration:

1. The model applies to HSRs that typically feature double tracks with an automatic block system.
2. The up and down directions of the HSR operate as independent systems, meaning they do

not influence each other. As a result, the impact from the opposite direction can be disregarded, allowing the focus to be on one direction. This paper examines the down direction.

3. All stations along the railway line are capable of handling train reception and departure simultaneously.
4. Two different speed classes of trains, medium and high speed, operate on the HSR line.
5. Overtaking occurs solely when high-speed trains overtake medium-speed trains.
6. The train timetable covers the entire operating day, excluding maintenance time windows.
7. Factors such as the number of high-speed multiple units in operation, as well as issues related to train joining and maintenance, are neglected.
8. All data required for solving the model are predetermined and known.

### 3.3 Definition of the Variables and Parameters

Before formulating the model, the variables and parameters used in the model are defined in Table 1.

**Table 1.**  
 Indices, Parameters and Variables in the Model

Notation	Definitions
$Xd_s^t$	Decision Variable, arrival time variable of train $t$ at station $s$
$Xf_s^t$	Decision Variable, departure time variable of train $t$ at station $s$
$S = \{1, 2, \dots, m\}$	Set of railway stations
$E = \{(u, v)   u, v \in S\}$	Set of intervals
$L = (S, E)$	Set of railway lines
$T = \{1, 2, \dots, n\}$	Set of trains
$tY_{uv}^t$	Pure running time for train $t$ in the interval $(u, v)$
$tQ_{uv}^t$	Starting additional time for train $t$ in the interval $(u, v)$ when it stops at station $u$
$tT_{uv}^t$	Stop additional time for train $t$ in the interval $(u, v)$ when it will stop at station $v$
$tmin_s^t$	Minimum dwell time for train $t$ at station $s$
$I_{uv}^D$	Minimum headway when the train will arrive the station $v$
$I_{uv}^E$	Minimum headway when the train enter the interval $(u, v)$ from the starting station
$Fs_{s0}^t$	The lower limit of the departure time for train $t$ at the starting station $s0$
$Fe_{s0}^t$	The upper limit of the departure time for train $t$ at the starting station $s0$
$TC_{uv}^S$	Starting time of skylight in the interval $(u, v)$
$TC_{uv}^E$	End time of skylight in the interval $(u, v)$
$DFX_s$	Number of arrival-departure track for down direction train reception and departure at station $s$
$m$	Any $m$ minute in a day
$\delta_s^t \in \{0, 1\}$	Binary variable for train stop, 1 if train $t$ stop at station $s$ , 0 otherwise
$\varphi_t \in \{0, 1\}$	Binary variable for train class, 1 if train belong to high-speed class, 0 otherwise

### 3.4 Constraints

A diverse set of constraints must be met to ensure the feasibility of the solution, including:

#### 3.4.1 Constraints of the Train Running Time in the Section

The constraints on train running time in a section refer to the difference between the train's arrival and departure times at a station. This difference equals the sum of the pure running time for the section, the additional starting time at the station, and the stopping time at the station. That is:

$$Xd_v^t - Xf_u^t = tY_{uv}^t + \delta_u^t tQ_{uv}^t + \delta_u^t tT_{uv}^t, (t \in T, u, v \in S, (u, v) \in E) \quad (1)$$

#### 3.4.2 Constraints of Dwell Time at Train Station

The dwell time of a train at a station must accommodate passenger boarding, alighting, and other essential tasks. When train  $t$  stops at station  $s$ , the dwell time should not be less than the minimum dwell time:

$$Xf_s^t - Xd_s^t \geq tmin_s^t, \quad (t \in T, s \in S) \quad (2)$$

### 3.4.3 Train Tracking Interval Time

For clarity, the tracking intervals are divided into sections, arrival (including arrival-to-arrival, arrival-to-through, through-to-arrival, and through-to-through), and departure intervals (including departure-to-departure, through-to-departure, departure-to-through, and through-to-through). Ensuring arrival and departure tracking intervals automatically satisfies the section tracking interval. Therefore, the departure and arrival times of adjacent leading train  $t_1$  and following train  $t_2$  when running in section  $(u, v)$  must satisfy.

$$Xf_u^{t_2} - Xf_u^{t_1} \geq I_{uv}^F, (t_1 \neq t_2, t_1, t_2 \in T, u, v \in S, (u, v) \in E) \quad (3)$$

$$Xd_v^{t_2} - Xd_v^{t_1} \geq I_{uv}^D, (t_1 \neq t_2, t_1, t_2 \in T, u, v \in S, (u, v) \in E) \quad (4)$$

### 3.4.4 Range Constraints of the Originating Train Departure Time

Trains should be scheduled to match the characteristics of passenger flow demand, which typically fluctuate and follow certain patterns during different time periods. Consequently, it is necessary to constrain train departure times within specific periods to align with peak and off-peak demand. This ensures that the number of trains operating corresponds to the passenger flow at different times, enhancing the efficiency and satisfaction of the rail service. Let  $sO$  be the origin station for train  $t$ , then the departure time of train  $t$  from station  $sO$  satisfies:

$$Fs_{sO}^t \leq Xf_{sO}^t \leq Fe_{sO}^t, (t \in T, sO \in S) \quad (5)$$

### 3.4.5 Constraints of Overtaking of Trains in the Same Direction

Overtaking trains can only occur at stations, and it is prohibited within sections. Therefore, for adjacent leading train  $t_1$  and following train  $t_2$  operating in section  $(u, v)$ , their departure and arrival times must satisfy:

$$(Xf_u^{t_2} - Xf_u^{t_1})(Xd_v^{t_2} - Xd_v^{t_1}) > 0, (t_1 \neq t_2 \text{ and } t_1, t_2 \in T; u, v \in S \text{ and } (u, v) \in E) \quad (6)$$

High-speed trains cannot be overtaken, thus the departure and arrival times of adjacent preceding medium-speed train  $t_1$  and following high-speed train  $t_2$  at station  $u$  must satisfy:

$$\varphi_{t_2}(Xd_u^{t_2} - Xd_u^{t_1})(Xf_u^{t_2} - Xf_u^{t_1}) > 0, (t_1 \neq t_2, t_1, t_2 \in T, u \in S) \quad (7)$$

It is stipulated that a medium-speed train can be overtaken at a station a maximum of two times. If a high-speed train overtakes a medium-speed train at a station, the overtaking must comply with the required train arrival and departure intervals both before and after the overtaking event.

### 3.4.6 Constraint of Receiving and Departure Track

During train operation, the number of trains stopping at a station at any given moment must not exceed the number of allocated receiving and departure tracks for those trains. Thus, at time  $t$ , the number of receiving and departure tracks occupied by trains at station  $s$  should satisfy the following condition:

$$\sum_{t \in T} [\omega(Xd_s^t, m) - \omega(Xf_s^t, m)] \leq DFX_s, (s \in S, 0 \leq m \leq 1440, m \in Z) \quad (8)$$

$$\text{Among them, the binary function } \omega(x, m) = \begin{cases} 1 & x \leq m \\ 0 & x > m \end{cases}$$

### 3.4.7 Constraint of Skylight

The skylight period for HSR in China is set from 00:00 to 06:00. The rectangular skylight for the following day, along with the interval type, can be selected based on the specific characteristics of the railway operation. Therefore, the arrival and departure times of train  $t$  when running between sections  $(u, v)$  should be outside the maintenance skylight:

$$Xd_v^t \leq TC_{uv}^S, (t \in T, u, v \in S, (u, v) \in E) \quad (9)$$

$$Xf_u^t \leq TC_{uv}^E, (t \in T, u, v \in S, (u, v) \in E) \quad (10)$$

### 3.5 Objective Function

As life becomes faster and living standards rise, the demand for HSR travel increases, along with higher expectations for high-speed rail services. Reducing train travel time not only meets passengers' needs for shorter journeys, making travel more convenient and efficient, but also improves train operational efficiency by reducing resource wastage. Therefore, the goal of optimization of this paper is to minimise the total travel time of the trains. Let  $s^O$  and  $s^D$  be the starting station and destination station of train  $t$ , respectively; then, the objective function expression for minimizing the total travel time of the train is:

$$\min Z = \sum_{t \in T} (Xd_{s^D}^t - Xf_{s^O}^t) \quad (11)$$

### 3.6 The Value of Key Parameters on Calculation Method of HSR Station Carrying Capacity

In HSR station carrying capacity analysis, the direct calculation method is used to determine the carrying capacity of receiving and departure tracks, while the utilization method is employed to calculate the carrying capacity of the throat area. Both methods are part of a comprehensive analysis approach. The formula for the comprehensive analysis method is given in the specification for HSR design as follows:

The capacity of receiving and departure tracks  $N_K$  refers to

$$N_K = \frac{M_k(1440 - T_t)(1 - \zeta_k^d)}{t_{zj}} \times K \quad (12)$$

$$t_{zj} = \alpha_{zf}t_{ZF} + \alpha_{tg}t_{TG} + \alpha_{sf}t_{SF} + \alpha_{zd}t_{ZD} + \alpha_{dk}t_{DK} \quad (13)$$

Where  $M_k$  are the number of receiving and departure tracks used for high-speed trains;  $T_t$  represents the time during which the railway station stops train reception and departure within a 24-hour period,  $\zeta_k^d$  stands for the idle coefficient of passenger train arrival and departure tracks, with a value range of 0.15-0.25.  $t_{zj}$  denotes the average time a passenger train occupies train arrival and departure track;  $K$  is the track utilization rate, typically ranging from 0.9 to 0.95.  $\alpha_{zf}$ ,  $\alpha_{tg}$ ,  $\alpha_{sf}$ ,  $\alpha_{zd}$ ,  $\alpha_{dk}$  denotes the proportion of turnaround, passing, starting, terminating, and arriving-departing trains relative to the total number of trains;  $t_{ZF}$ ,  $t_{TG}$ ,  $t_{SF}$ ,  $t_{ZD}$ ,  $t_{DK}$  denotes the average time each turnaround, passing, starting, terminating, and arrival-departure train occupies receiving and departure track.

Utilization rate of the throat turnout group for the entire day is formulated as follows:

$$K_{Throat}^{Day} = \frac{T_{Throat}^{Day} - \sum t_g}{(1440 - T_t - \sum t_g)(1 - \zeta_k^{Day})} \quad (14)$$

Where  $T_{Throat}^{Day}$  denotes the total occupation time of the throat turnout group throughout the day;

$\zeta_k^{Day}$  denotes the vacancy coefficient of the turnout group, typically ranging from 0.2 to 0.3;

$\sum t_g$  represents the fixed operational time of the turnout group. The throughput capacity

utilization rate of the throat turnout group during the peak period, can be formulated as

$$K_{Throat}^P = \frac{T_{Throat}^P - \sum t_g}{(T_P - \sum t_g)(1 - \zeta_k^P)} \quad (15)$$

Where  $T_{Throat}^P$  denotes the total occupation time of the throat turnout group during the peak period;

$\zeta_k^P$  represents the vacancy coefficient of the throat turnout group, typically taken as 0.1;

$T_P$  is the duration of the peak period.

The carrying capacity of the throat turnout group is formulated as follow:

$$N_{Throat}^i = \frac{n^i}{K_{Throat}} \quad (16)$$

Where  $n^i$  denotes the number of passenger trains in the  $i$  direction included in the calculation;  $K_{Throat}$  represents the utilization rate of the throat turnout group either throughout the day or during the peak period.

The comprehensive analysis method, in essence, involves deducing the carrying capacity under saturated operational conditions based on existing operational data. This approach is widely adopted due to its simplicity and practicality, and it has demonstrated effective results in practical applications. However, as its calculation principles are derived from those used for conventional railway stations, the method has exhibited certain limitations in adapting to the rapid development of HSR in China in recent years. These limitations have become increasingly apparent during the research process, highlighting the need for a more tailored and refined approach. Specifically, inconsistencies exist between the calculation methods outlined in the current HSR design specifications and the operational principles of the HSR CTC system. These discrepancies manifest in the following three key aspects:

1. **Variability in Train Occupancy Times on Arrival/Departure Tracks:** The specifications provide standardised occupancy times for arrival and departure tracks, differentiated by speed class. However, due to variations in station layouts, differences in throat lengths, and diverse running times within throat areas, the actual occupancy times of arrival and departure tracks vary significantly. This is particularly evident in the differences between originating/terminating stations and intermediate stations, where train types and operational times differ considerably. Applying a uniform standard to calculate capacity fails to account for the unique characteristics and operational variations among different stations.

2. **Segmentation of Throat Areas Based on Track Circuits:** The throat areas of HSR stations are divided into segments based on different track circuits, which render the original calculation methods inconsistent with actual operational practices at railway sites. This segmentation complicates the application of traditional methods, as they do not align with the dynamic and segmented nature of HSR operations.

3. **Concentration of Passenger Demand During Daylight Hours:** Unlike conventional railways, passenger demand on HSRs is predominantly concentrated during daylight hours. As a result, the first passenger train departing from a station often does not directly follow the triangular section after the maintenance window, and the last passenger train arriving at the station during the day is not typically positioned immediately before the triangular section preceding the maintenance window. This operational pattern necessitates a more nuanced approach to categorising trains based on their specific operational processes at HSR stations.

In light of these discrepancies, it is evident that the conventional methods for calculating carrying capacity, while effective for traditional railways, are not fully suited to the unique operational



characteristics of HSR systems. A more refined approach is required, one that accounts for the specificities of HSR station layouts, operational processes, and passenger demand patterns. By categorising trains based on their operational roles and studying their occupancy times separately, it becomes possible to develop a more accurate and dynamic method for calculating HSR station capacity, thereby enhancing the overall efficiency and reliability of the HSR network.

The process of terminating trains occupying the receiving and departure track is illustrated in Figure 1. The time occupied by trains terminating the receiving and departure track can be formulated as follows:

$$t_{ZD} = t_{Pr} + t_{Th}^{in} + t_{Cst} + t_{Sdw} + t_{at}^{Eip} + t_{Rtb} \quad (17)$$

$t_{Pr}$  refers to the time from initiation of the train receiving route to the moment the front of the train passes the home signal.  $t_{Th}^{in}$  denotes the duration during which the train occupies the throat area at the station entrance.  $t_{Cst}$  denotes the time from when the train's rear end completely enters the track to the point when the train comes to a stop.  $t_{Sdw}$  is the dwell time at the railway station.  $t_{at}^{Eip}$  represents the time from the train's initiation of movement (in preparation for entering high-speed train depot) to the point when the rear end of the train passes the departure signal.  $t_{Rtb}$  refers to the time between the CTC system's confirmation that all devices related to the route have been cleared and the initiation of the next route trial.

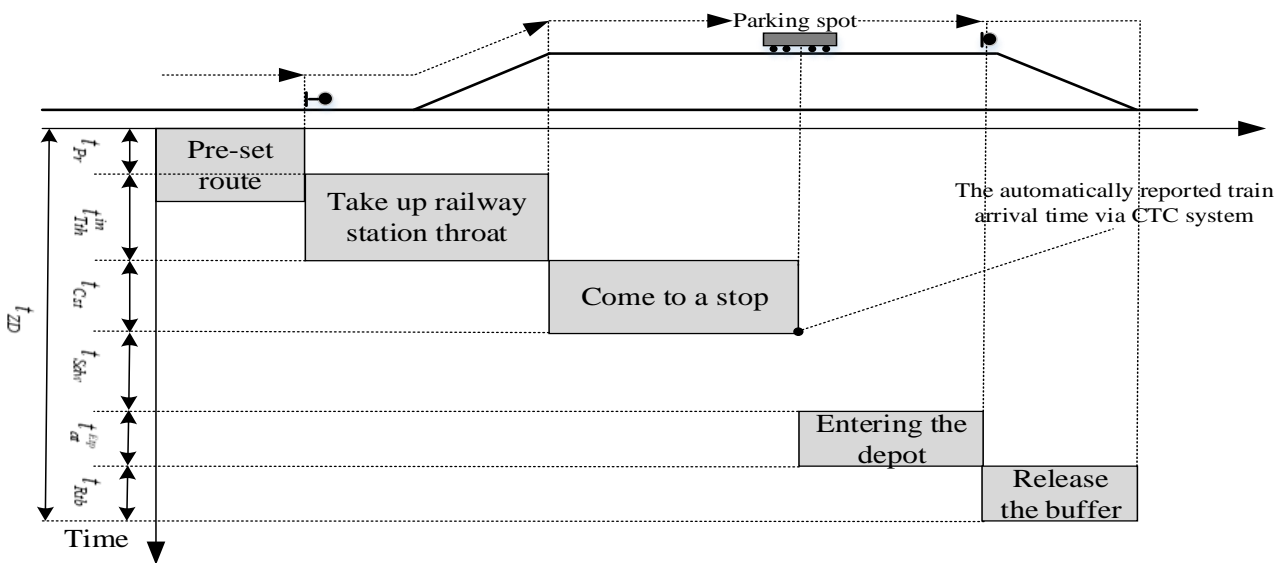
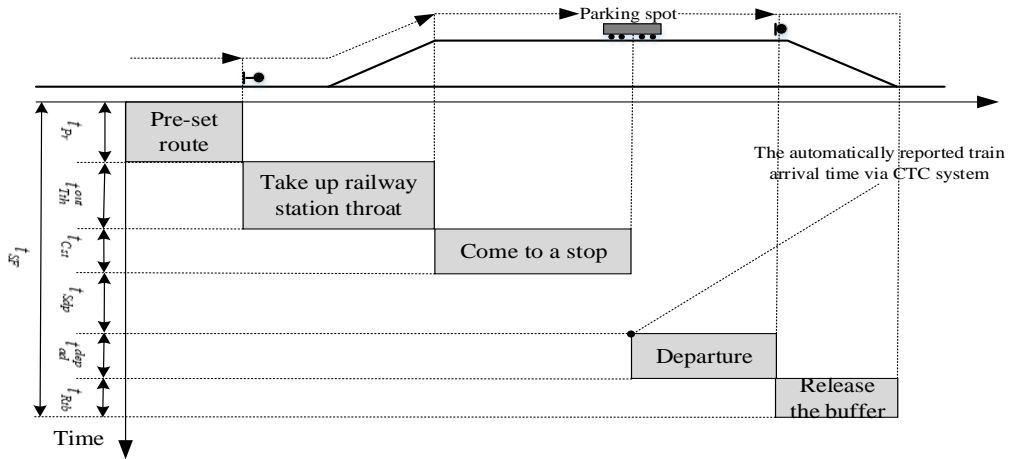


Fig. 1. Time Occupied by Arriving Trains on Receiving-Departure Track

The process of originating trains occupying the arrival and departure track is illustrated in Figure 2. The time occupied by originating trains on the arrival/departure track can be formulated as follows:

$$t_{SF} = t_{Pr} + t_{Th}^{out} + t_{Cst} + t_{Sdp} + t_{ad}^{dep} + t_{Rtb} \quad (18)$$

Where  $t_{Th}^{out}$  refers to the time during which the train occupies the throat area upon departure from the high-speed train depot.  $t_{Sdp}$  denotes the duration from the moment the train comes to a stop on the arrival/departure track until it starts moving for departure.  $t_{ad}^{dep}$  represents the time from the initiation of the train's departure to the point when the rear of the train passes the station departure signal.



**Fig. 2.** Time Occupied by Originating Trains on Receiving-Departure Track

The process of arrival-departure trains occupying the arrival and departure track is illustrated in Figure 3. The time occupied by these trains on the arrival and departure track can be formulated as follows:

$$t_{DK} = t_{Pr} + t_{Th}^{in} + t_{Cst} + t_{Sdw} + t_{ad}^{dep} + t_{Rtb} \quad (19)$$

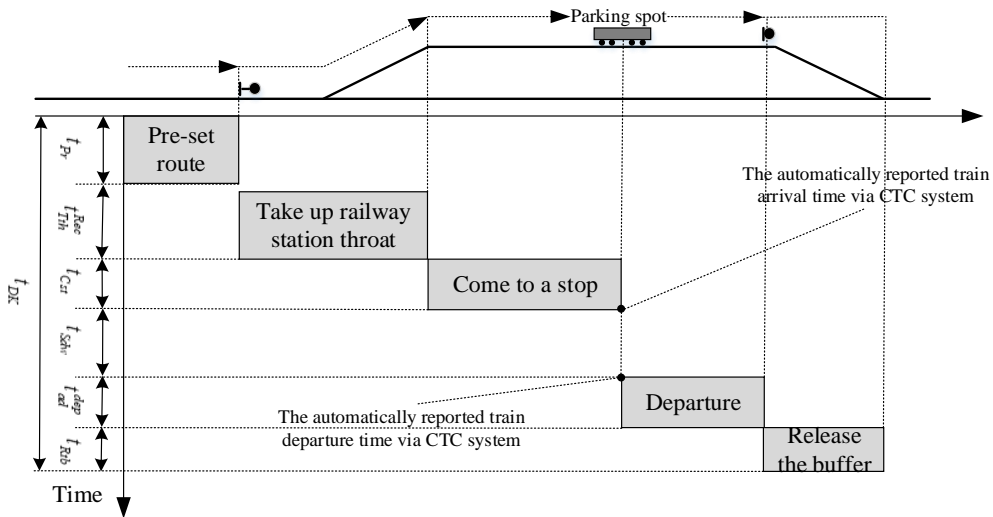


**Fig. 3.** Time Occupied by Arrival-Departure Trains on Receiving-Departure Track

The time occupied by turnaround trains on the arrival and departure track can be formulated as follow:

$$t_{ZF} = t_{Pr} + t_{Th}^{in} + t_{Cst} + t_{Sdw} + t_{ad}^{dep} + t_{Rtb} \quad (20)$$

The time occupied by passing trains on the arrival and departure track can be formulated as follow:

$$t_{TG} = t_{Pr} + t_{through} + t_{Rtb} \quad (21)$$

where  $t_{through}$  denotes the time from when the front of the train passes the home signal to when the rear of the train passes the station departure signal.

#### 4. Algorithm

When solving the high-speed train timetable design problem, the section and train operation sequence can be encoded to form a chromosome. During the decoding process, the train arrival

and departure times are calculated based on the operation sequence. The optimal section-train operation sequence obtained through the genetic algorithm is then decoded to produce the optimal train timetable.

#### 4.1 Encoding

This paper employs a two-dimensional sorted integer encoding method, using a matrix of size  $m \times n$  to represent the running order of  $n$  trains across  $m$  intervals. Figure 4 illustrates the structure of a single chromosome, where the third row of the matrix indicates that the running order of trains on the third interval is Train 1, 5, 3, 6, 4, and 2. If certain gene values representing train numbers appear outside the sections between originating and terminal stations, they are considered invalid genes. During the decoding process, these invalid genes should be disregarded, and only the valid genes should be decoded.

$$A_{4 \times 6} = \begin{bmatrix} 1 & 5 & 3 & 6 & 4 & 2 \\ 1 & 5 & 3 & 6 & 4 & 2 \\ 1 & 5 & 3 & 6 & 4 & 2 \\ 1 & 5 & 3 & 6 & 4 & 2 \end{bmatrix}$$

Fig. 4. Schematic Diagram of Chromosome Structure

#### 4.2 Decoding Algorithm

The chromosome encodes the train operation sequence within each section, which necessitates decoding operations to obtain the train timetable. Once decoded, the specific arrival and departure times of the trains are used to calculate the fitness function value. The layout of the train path must adhere to the constraints in the model, ensuring that it satisfies not only the operational requirements of the current train ( $t_2$ ) but also avoids conflicts with the preceding train ( $t_1$ ). The departure time of train  $t_2$  from the starting station of interval ( $u, v$ ) must meet the following requirements:

Satisfy the constraint of dwell time:  $Xf_u^{t_2'} = Xd_u^{t_2} + \delta_u^{t_2} \times tmin_u^{t_2}$ .

Satisfy the constraint of departure interval:  $Xf_u^{t_2''} = Xf_u^{t_1} + I_{uv}^F$ .

Satisfy the constraint of arrival interval:  $Xf_u^{t_2'''} = Xf_v^{t_1} + I_{uv}^D - (tY_{uv}^{t_2} + \delta_u^{t_2} tQ_{uv}^{t_2} + \delta_v^{t_2} tT_{uv}^{t_2})$

Satisfy range of starting time:  $Xf_u^{t_2''''} \leq t_{so}$ .

In conclusion, the formula for calculating the departure time of train  $t_2$  from the starting station of the section ( $u, v$ ) is:

$$Xf_u^{t_2} = \begin{cases} TC_{uv}^E \text{ (end time of skylight) } & \text{the first train in the section (originating)} \\ Xf_u^{t_2'} & \text{the first train in the section (non - originating)} \\ \max\{Xf_u^{t_2''}, Xf_u^{t_2'''}, Xf_u^{t_2''''}\} & \\ \max\{Xf_u^{t_2'}, Xf_u^{t_2''}, Xf_u^{t_2'''}\} & \text{non - originating train in the section} \end{cases} \quad (22)$$

In equation (22), if  $Xf_u^{t_2} = Xf_u^{t_2''}$ , it indicates that there is at least a departure interval conflict. The conflict resolution time  $\Delta T = Xf_u^{t_2'} - Xf_u^{t_2''}$ . If  $Xf_u^{t_2} = Xf_u^{t_2''}$ , it indicates that there is at least an arrival interval conflict. The conflict resolution time  $\Delta T = Xf_u^{t_2'} - Xf_u^{t_2''}$ . If  $Xf_u^{t_2} = Xf_u^{t_2'}$ , it does not indicate a conflict between trains, but only that the initial train needs to meet the requirements of the departure time. At this point, conflict resolution is not needed.

The train  $t$ 's arrival time at the terminal station of the section ( $u, v$ ) is calculated according to

the running time of the section, and the formula is:

$$Xd_v^t = Xf_u^t + tY_{uv}^t + \delta_u^t t Q_{uv}^t + \delta_v^t t T_{uv}^t \quad (23)$$

Assuming the number of sections is m and the number of trains is n, the design of the train path follows the principle of breadth-first cyclic routing. The specific steps for decoding the design are as follows:

Step 1: Set  $i = 0, j = 0$ .

Step 2: Take train j within interval i. If it is a valid gene, go to step 3; otherwise, go to step 6.

Step 3: Calculate the departure time of the train according to equation (22). If the train is neither the first in the interval nor the first train in the section, proceed to step 4. Otherwise, proceed to step 5.

Step 4: Resolve conflicts. If  $Xf_u^{t_2} = Xf_u^{t_2''}$ , it indicates that there is at least a departure interval conflict, proceed to step 4.1; if  $Xf_u^{t_2} = Xf_u^{t_2'''}$ , it indicates that there is at least an arrival interval conflict, proceed to step 4.2.

Step 4.1: Resolve departure interval conflicts. During conflict resolution,  $\Delta T = Xf_u^{t_2''} - Xf_u^{t_2}$ . Move all affected operation lines within the 0 to i-1 interval backward by  $\Delta T$ .

Step 4.2: Resolve arrival interval conflicts. During conflict resolution,  $\Delta T = Xf_u^{t_2'''} - Xf_u^{t_2}$ . Move all affected operation lines within the 0 to i-1 interval backward by  $\Delta T$ .

Step 5: Calculate the arrival time of the train according to equation (23), based on the running time within the interval.

Step 6: Set  $j=j +1$ , check if  $j \geq n$  is true. If so, go to step 7; otherwise, go back to step 2.

Step 7: Set  $i=i+1, j = 0$ , check if  $i \geq m$  is true. If so, go to step 8; otherwise, go back to step 2.

Step 8: Check if the other constraints are satisfied. If all constraints are met, output the solution as feasible.

The train path that needs to be moved when there is a conflict between the departure and arrival intervals in steps 4.1 and 4.2 is shown in Figures 5 and 6. The circled text in the figures represents the train that has a conflict between the arrival and departure intervals, and the coloured grid at the bottom indicates the train's running line that needs to be moved backwards. The decoding process flowchart is shown in Figure 7.

0	1	2	3
0	2	1	3
0	②		

Fig. 5. High-Speed Trains Running Lines When Resolving Conflicts

0	1	2	3
0	2	1	3
0	2	①	

Fig. 6. Medium Trains Running Lines When Resolving Conflict

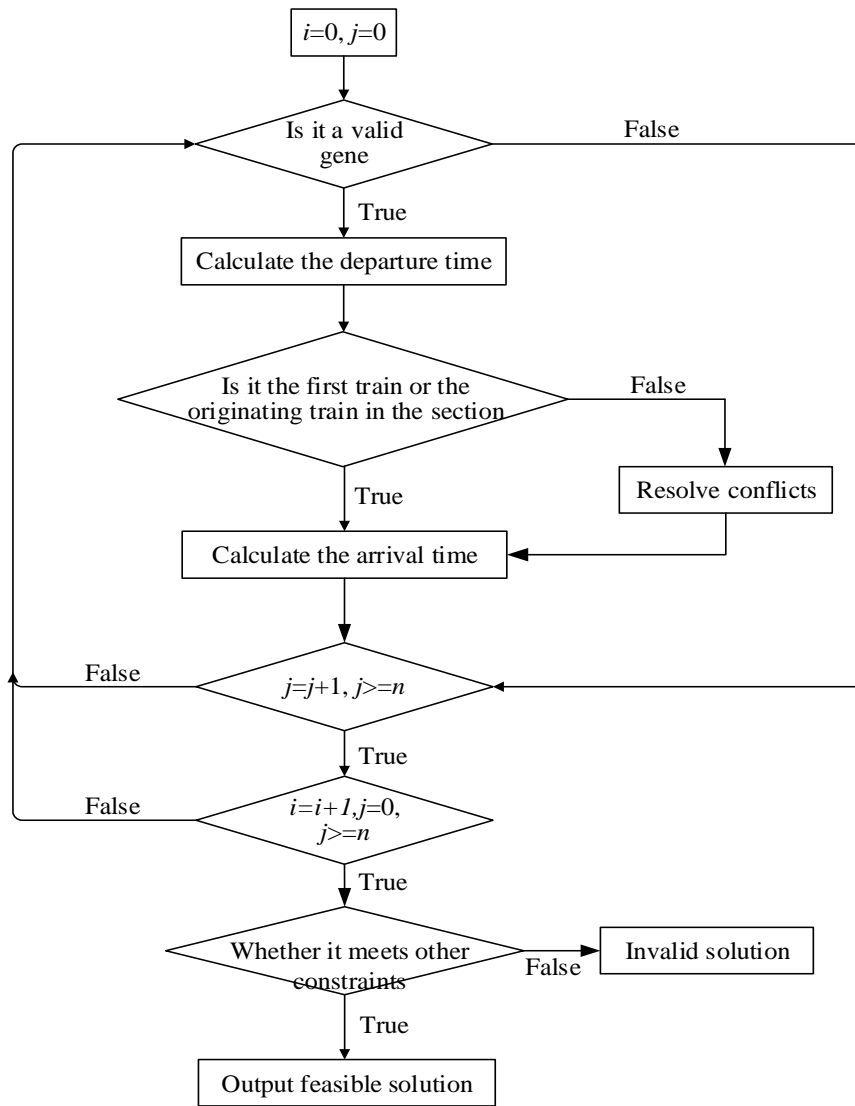


Fig. 7. Decoding Process

### 4.3 Fitness Function

The genetic algorithm does not rely on external information but uses the value of the fitness function (a modified version of the objective function) to evaluate the individual's quality and select individuals. When employing roulette wheel selection, the probability cannot be negative. As this paper addresses a minimisation problem, the fitness function is set as the reciprocal of the objective function, that is:

$$Fit\_F(x) = \frac{1}{Z} = \frac{1}{\sum_{t \in T} (Xd_{sD}^t - Xf_{sO}^t)} \quad (24)$$

### 4.4 GA operators

#### 4.4.1 Selection

For selection, this paper combines the elitism strategy with the roulette wheel method. The best individual is copied to a new population, and the roulette wheel method is used to select from the current population. The higher an individual's fitness, the larger its section on the wheel and its probability of being chosen. Figure 8 shows a simple roulette wheel with a total area of 10, where individuals 1, 2, 3, and 4 occupy areas (fitness) of 4, 2, 1, and 3, respectively. Thus, the order

of selection is: individual 1, 4, 2, 3.

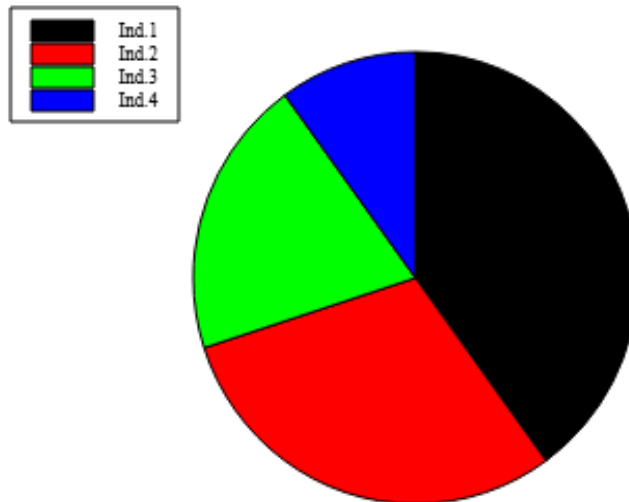


Fig. 8. Roulette Wheel Diagram

#### 4.4.2 Crossover

This paper uses a two-dimensional sorted integer coding method to represent the running order of trains in each interval. During the crossover operation, it is essential to maintain the rationality of the coding, ensuring that each train appears only once in each interval. To achieve this, the ordered crossover method is employed, which preserves both rationality and a good adjacent relationship. The specific steps of the ordered crossover are as follows:

Step 1: First, traverse the population individuals as parent 1, and randomly select a crossover position in parent 1 (Figure 9).

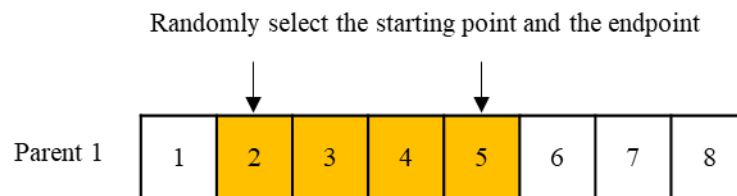


Fig. 9. Select Crossover Points

Step 2: Fill the genes 2, 3, 4, and 5 from the crossover position in parent 1 into the corresponding positions in offspring 1 (Figure 10).



Fig. 10. Copy the Genes at the Crossover Positions

Step 3: Randomly select parent 2 from the population, skip the existing genes in offspring 1, and sequentially fill the blank spaces in offspring 1 with the remaining genes 8, 1, 7, and 6 (Figure 11).

Finally, the offspring obtained is child1 = [8,2,3,4,5,1,7,6].

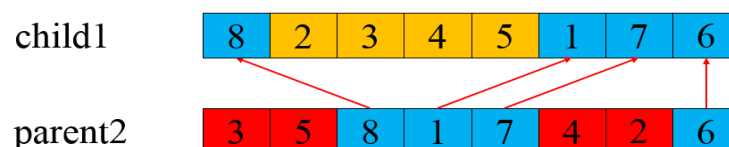


Fig. 11. Place the Remaining Genes

#### 4.4.3 Mutation

To ensure the rationality of individual coding, this paper adopts the exchange mutation method. The process involves randomly selecting mutation positions in chromosomes and determining whether to swap their corresponding positions based on the mutation probability. In the mutation process shown in Figure 9, gene 2 and gene 7 are swapped (Figure 12).

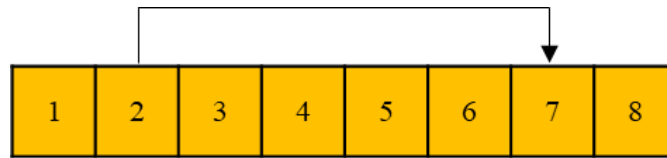


Fig. 12. Gene Exchange Process

#### 4.5 Algorithm design

The algorithm for solving the problem of high-speed train timetable compilation using genetic algorithm is as follows.

Step 1: Enter the data required for the model and initialise the algorithm parameters. The parameters needed include line and train data, as well as the basic elements of the train timetable, etc. The algorithm parameters include population size  $M$ , number of iterations  $N$ , crossover probability  $P_c$ , mutation probability  $P_m$ .

Step 2: Let  $n=0$ , randomly generate an initial population  $p(0)$  consisting of  $M$  individuals.

Step 3: Determine whether the termination condition ( $n>N$ ) has been met. If so, go to step 10; Otherwise, go to step 4.

Step 4: Calculate the fitness of contemporary individuals according to equation (14).

Step 5: Select the Operation: Firstly, copy the  $K$  individuals with the highest fitness in population  $p(n)$  into the next generation population  $p(n+1)$ , and then select  $p(n)$  using the roulette wheel method. Repeat this operation until a temporary population  $p^{(n)'}$  consisting of  $M-K$  individuals is generated.

Step 6: Crossover: Select two parents from  $p^{(n)'}$  and generate  $\delta \in [0,1]$ . If  $p_c > \delta$ , perform the crossover. Repeat this operation until a temporary population  $p^{(n)''}$  consisting of  $M-K$  feasible individuals is generated.

Step 7: Mutation: Select an individual from  $p^{(n)''}$  and generate  $\gamma \in [0,1]$ . If  $p_m > \gamma$ , then perform the mutation. Repeat this operation until a temporary population  $p^{(n)'''}$  consisting of  $M-K$  feasible individuals is generated.

Step 8: Copy the temporary population  $p^{(n)'''}$  into the next generation population  $p(n+1)$ .

Step 9: Set  $n = n + 1$ , go to step 3.

Step 10: Output the optimal individual  $p_{max}$ .

### 5. Computational Experiments

#### 5.1 An Overview of Shanghai-Hangzhou HSR

The Shanghai-Hangzhou HSR runs from Shanghai Hongqiao Station to Hangzhou East Station, covering a main line length of approximately 159 kilometres, with a designed maximum speed of 350 kilometres per hour (as shown in Figure 13). The route includes 9 stations handling passenger services. These stations are Shanghai Hongqiao, Songjiang South, Jinshan North, Jiashan South, Jiangxing South, Tongxiang, Haining West, Linping South, and Hangzhou East. The section information is detailed in Table 2, where the pure running time for each section is calculated by rounding down the mileage divided by the operating speed.



Fig. 13. Shanghai-Hangzhou High Speed Railway

Table 2.  
 Section Information of Shanghai-Hangzhou High speed Railway

No.	Section	Distance (km)	Pure Running Time (min)	
			G (300km/h)	D (250km/h)
1	Shanghai Hongqiao—Songjiang South	31	6	7
2	Songjiang South—Jinshan North	17	3	4
3	Jinshan North—Jiashan South	19	4	5
4	Jiashan South—Jiaxing South	17	3	4
5	Jiaxing South—Tongxiang	28	6	7
6	Tongxiang—Haining West	21	4	5
7	Haining West—Liping South	11	2	3
8	Liping South—Hangzhou East	15	3	4

The train set consists of 94 trains, including 81 G-class trains and 13 D-class trains, all operating from Shanghai Hongqiao Station to Hangzhou East Station. The stopping plans at stations are based on the current stop times at each station along the Shanghai-Hangzhou HSR, as shown in Table 3. Moreover, referring to the current dispatch headway of the Shanghai-Hangzhou HSR line, the number of departure trains for each period is designed as shown in Table 4.

Table 3.  
 Railway Station Stopping Plan

No.	Railway Station									Number of Trains
	Shanghai Hongqiao	Songjiang South	Jinshan North	Jiashan South	Jiaxing South	Tongxiang	Haining West	Liping South	Hanzhou East	
1	1	0	0	0	0	0	0	0	1	15
2	1	0	0	0	1	0	0	0	1	12
3	1	0	0	0	1	0	1	0	1	10
4	1	0	0	0	1	0	0	1	1	8
5	1	0	0	0	1	1	0	0	1	6
6	1	0	0	1	1	0	0	0	1	6
7	1	0	1	0	1	0	0	0	1	5
8	1	0	0	1	0	1	0	0	1	5
9	1	1	0	0	1	0	0	0	1	4
10	1	0	1	0	1	0	1	0	1	3



11 1	0	1	0	1	0	0	1	1	2
12 1	1	0	1	1	0	0	0	1	2
13 1	0	1	0	1	1	0	0	1	2
14 1	1	0	0	0	1	0	0	1	2
15 1	0	0	0	0	1	0	1	1	1
16 1	0	0	0	0	0	0	1	1	1
17 1	0	0	1	0	0	1	0	1	1
18 1	1	0	0	1	0	1	0	1	1
19 1	1	0	0	0	0	0	1	1	1
20 1	0	0	0	1	1	0	1	1	1
21 1	0	0	1	1	0	1	1	1	1
22 1	0	0	1	0	1	1	0	1	1
23 1	1	0	0	1	0	0	1	1	1
24 1	0	0	1	0	1	0	1	1	1
25 1	0	0	1	0	0	0	0	1	1
26 1	0	0	0	1	0	1	1	1	1

**Table 4.**  
 Number of Departure Trains in Each Period

Period	Number of Trains	Period	Number of Trains
6:00-7:00	10	14:00-15:00	5
7:00-8:00	9	15:00-16:00	9
8:00-9:00	6	16:00-17:00	6
9:00-10:00	4	17:00-18:00	6
10:00-11:00	5	18:00-19:00	4
11:00-12:00	4	19:00-20:00	7
12:00-13:00	6	20:00-21:00	4
13:00-14:00	7	21:00-22:00	2

The number of main lines and receiving and departure tracks at the railway stations along the Shanghai Hongqiao-Hangzhou East HSR is shown in Table 5.

**Table 5.**  
 The Number of Main Lines and Receiving and Departure Tracks along the Shanghai Hongqiao-Hangzhou East HSR

No.	Station	Number of Main Line	Number of Receiving Departure Track
1	Shanghai Hongqiao	2	17
2	Songjiang South	2	2
3	Jinshan North	2	2
4	Jiashan South	2	2
5	Jiaxing South	2	6
6	Tongxiang	2	2
7	Haining West	2	2
8	Hangzhou East	2	12

Moreover, the carrying capacity calculation parameters for the receiving and departure tracks at Hangzhou East station can be obtained based on CTC data. Due to the large number of parameters for all stations, it is impractical to list them here, so they are omitted (Table 6).

**Table 6.**  
 Parameter Value of Carrying Capacity Calculation

Parameter	Value	Parameter	Value
$l_{Pr}$	2 min	$l_{at}$	0.5 min
$l_{Th}$	2	$l_{Cst}$	0.72 min
$l_{Tth}$	2	$l_{Rtb}$	0.1 min
$l_{ad}$	0.5min	$l_t$	387 min

### 5.2 Example

Other required data are shown in Table 7. Moreover, the settings of the genetic algorithm parameters are shown in Table 8. The algorithm was implemented using Python programming to generate a train timetable, where the arrival and departure times of trains are represented in integer minutes. The visualised train timetable, created using the plot() function, is shown in Figure 11. The centre line of the station in the running diagram is determined by the ratio of running time between sections, with time divided by vertical lines in hours. Passenger trains are depicted by a red line, while trains starting with the letter D are displayed in blue for clearer visualisation.

**Table 7.**  
Other Input Parameters

Parameters	Parameter Value
D-train Additional Starting Time	1 min
D-train Stopping Additional Time	1 min
G-train Additional Starting Time	2 min
G-train Stopping Additional Time	2 min
Minimum Dwell Time	2 min
Minimum Arrival Tracking Interval Time	3 min
Minimum Departure Tracking Interval Time	5 min
Starting Time of Skylight <sup>1</sup>	0 min
End Time of Skylight	360 min
Quantity of Receiving Arrival-Departure Track at Each Railway Station	2

<sup>1</sup>This refers to the time reserved for construction and maintenance work by not plotting train path or adjusting/reducing train operations in the train timetable.

**Table 8.**  
Parameters of Genetic Algorithm

Parameters of GA	Parameter Value
Population Size $M$	80
Evolutionary Generations $N$	300
Crossover Probability $P_c$	0.8
Mutation Probability $P_m$	0.05

### 5.3 Model Architecture

The train timetable in Figure 14 visually shows the operational status of trains at various stations. The train path arrangement is dense, with higher densities from 6:00 AM to 9:00 AM and 4:00 PM to 6:00 PM, reflecting peak travel times. No conflicts exist, ensuring operations and safety intervals are met, making it a feasible and conflict-free timetable. The G-trains follow the plan, with travel times matching the schedule. D-trains, however, extend their stopping times to avoid G-trains or accommodate arrival/departure intervals, resulting in slightly longer travel times. The total travel time is 4325 minutes, 39 minutes longer than the ideal 4286 minutes, which assumes completely independent train operations. The model still faces discrepancies compared to reality, where increased network complexity and more constraints often lead to longer travel times, highlighting the challenge of creating a realistic operation diagram.

The train path in this study is relatively dense. The G-train runs as planned, with travel times matching the schedule. However, the D-train extends its stopping time to avoid the G-train or meet arrival and departure intervals, leading to a slight increase in travel time, as expected. The total travel time of the timetable is 4325 minutes, compared to the planned 4286 minutes, which assumes completely independent train operations. The real timetable is 39 minutes longer than the planned one. Given the receiving and departure track utilisation rate, achieving the ideal travel time is difficult. The model in this paper still shows some gaps compared to reality, where network

complexity and additional factors impose more constraints, often resulting in longer travel times. This highlights the scale and complexity of the train timetable problem.

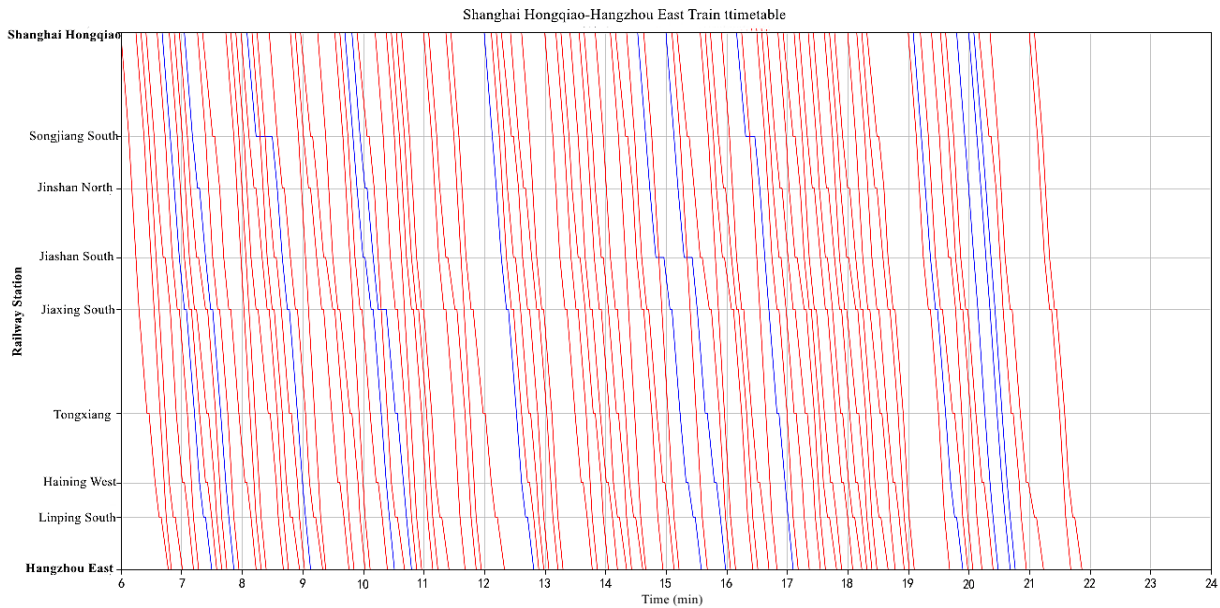


**Fig. 14.** Result Train Timetable of Shanghai Hongqiao to Hangzhou East Railway

The train timetable is evaluated using both quantitative and qualitative indices. As this study does not consider high-speed train connections, quality indices like connection times are excluded. Other relevant evaluation indices for the train timetable are shown in Table 9. From the quality index, it is evident that although the G-train adheres to the planned schedule, its average speed significantly differs from the target of 300 km/h. This discrepancy arises because the stations on the railway line are relatively close, and the train’s pure running time is short. Consequently, the time spent accelerating and decelerating has a more substantial impact on the overall travel time. The portion of time spent running at 300 km/h is relatively small, leading to a lower average speed and technical speed. For D-trains, in addition to these factors, the average speed may further decrease due to the need to avoid G-trains or extend stopping times to accommodate arrival and departure intervals.

**Table 9.**

Evaluation Index of Train Timetable

Train Type	Quantity Index		Quality Index	
	Quantity of Train	Train Running Kilometres	Average Technical Speed	Average Travel Speed
G	81	12879	228 km/h	211 km/h
D	13	2067	200 km/h	186 km/h
G and D	94	14946	224 km/h	207 km/h

## 6. Conclusion and Future Research

At present, in the process of formulating HSR timetables in China, foundational data for newly opened lines is primarily provided by departments such as track maintenance, signalling, and power supply, while operational parameters are supplied by the locomotive department. These parameters are predominantly determined using reference standards, with field testing employed for calibration. The final parameter values are often derived based on past experience. However, this approach rarely accounts for the specific characteristics of station equipment and operations, resulting in broad and imprecise parameter values. This research seeks to address this gap by examining the determination of key parameters in the comprehensive analysis method, including

train occupancy time on arrival and departure tracks, train occupancy time in throat areas, and daily idle time. The study refines and standardises the values of these parameters. Subsequently, this paper establishes a single-objective optimisation model for HSR train timetabling and applies a genetic algorithm to solve the model, demonstrating a certain level of feasibility. Nevertheless, the model developed in this paper still differs significantly from the actual complex and dynamic conditions, as many practical factors have not been considered. Additionally, the study has several limitations, and future research could address the following aspects:

1. Incorporation of Practical Factors: In the process of establishing and solving the model, this paper deliberately omits issues such as train connections and passenger transfers, resulting in an insufficient consideration of real-world conditions. Furthermore, the model only uses total travel time as the optimisation objective, making the evaluation of train schedule quality overly simplistic and narrow. Therefore, future work could consider incorporating more practical factors, such as passenger transfer times, train connection constraints, and operational flexibility, into the model to enhance its real-world applicability and robustness.

2. Exploration of Alternative Solution Methods: While this paper employs the widely used genetic algorithm for solving scheduling problems, numerous traditional methods are also available for this task. Thus, it would be worthwhile to explore alternative methods for solving the train scheduling problem, comparing their effectiveness, efficiency, and adaptability to complex operational scenarios.

### Author Contributions

Conceptualization, C.C.; methodology, W.L.; software, W.L.; validation, W.L.; formal analysis, W.L.; investigation, W.L.; resources, W.L.; data curation, W.L.; writing—original draft preparation, C.C. and W.L.; writing—review and editing, C.C.; visualization, C.C.; supervision, C.C.; project administration, C.C.; funding acquisition, C.C. All authors have read and agreed to the published version of the manuscript.

### Data Availability Statement

The data used to support the findings of this study are available from the corresponding author upon request.

### Conflicts of Interest

The authors declare that they have no conflicts of interest.

### Acknowledgement

The authors gratefully acknowledge the editor and the anonymous reviewers for their valuable comments on an earlier draft of this manuscript. Their suggestions significantly improve this paper. This work was supported by Hunan Provincial Department of Education Scientific Research Project (Grant No.23C0814).

### References

- [1] China, N. (2014). Code for design of high speed railway. *China Ministry of Railways, TB*, 10621-2014.
- [2] Serafini, P. and W. Ukovich. (1989). A mathematical model for periodic scheduling problems. *SIAM Journal on Discrete Mathematics*, 2(4), 550-581. <https://doi.org/10.1137/0402049>
- [3] Schrijver, A. and A. Steenbeek, *Dienstregelingontwikkeling voor Railned (timetable*

- construction for Railed). 1994, Technical report, CWI, Center for Mathematics and Computer Science ....
- [4] Mbah, O. and Q. Zeeshan. (2023). Optimizing path planning for smart vehicles: a comprehensive review of metaheuristic algorithms. *J Eng Manage Syst Eng*, 2(4), 231-271. <https://doi.org/10.56578/jemse020405>
- [5] Odijk, M.A. (1996). A constraint generation algorithm for the construction of periodic railway timetables. *Transportation Research Part B: Methodological*, 30(6), 455-464. [https://doi.org/10.1016/0191-2615\(96\)00005-7](https://doi.org/10.1016/0191-2615(96)00005-7)
- [6] El Chaal, R., S. Boucheфра, and M. Aboutafail. (2023). Stochastic dynamics and extinction time in SIR epidemiological models. *Acadlore Trans. Appl Math. Stat*, 1(3), 181-202. <https://doi.org/10.56578/atams010305>
- [7] Li, K., H. Huang, and P. Schonfeld. (2018). Metro Timetabling for Time-Varying Passenger Demand and Congestion at Stations. *Journal of Advanced Transportation*, 2018(1), 3690603. <https://doi.org/10.1155/2018/3690603>
- [8] Wang, Y., et al. (2015). Passenger-demands-oriented train scheduling for an urban rail transit network. *Transportation Research Part C: Emerging Technologies*, 60, 1-23. <https://doi.org/10.1016/j.trc.2015.07.012>
- [9] Shi, F., et al. (2012). Optimization method for train diagram of high-speed railway considering the turnover of multiple units and the utilization of arrival-departure tracks. *Zhongguo Tiedao Kexue*, 33(2), 107-114.
- [10] Zhou, X. and M. Zhong. (2007). Single-track train timetabling with guaranteed optimality: Branch-and-bound algorithms with enhanced lower bounds. *Transportation Research Part B: Methodological*, 41(3), 320-341. <https://doi.org/10.1016/j.trb.2006.05.003>
- [11] Berbiche, N., et al. (2024). An Integrated Inventory-Production-Distribution Model for Crisis Relief Supply Chain Optimization: A Systematic Review and Mixed Integer Programming Formulation. *Journal Européen des Systèmes Automatisés*, 57(3). <https://doi.org/10.18280/jesa.570329>
- [12] Lu, C., L. Zhou, and R. Chen. (2018). Optimization of high-speed railway timetabling based on maximum utilization of railway capacity. *J. Railw. Sci. Eng*, 15(11), 2746-2754.
- [13] Higgins, A., E. Kozan, and L. Ferreira. (1996). Optimal scheduling of trains on a single line track. *Transportation research part B: Methodological*, 30(2), 147-161. [https://doi.org/10.1016/0191-2615\(95\)00022-4](https://doi.org/10.1016/0191-2615(95)00022-4)
- [14] Muniasamy, K., P. Venugopal, and G. Pakkirisamy. (2023). Genetic Algorithm-Driven Optimization of Scheduling and Preventive Measures in Parallel Machines. *Mathematical Modelling of Engineering Problems*, 10(5). <https://doi.org/10.18280/mmep.100533>
- [15] Du, Y., et al. (2024). An investigation into multi-stage, variable-batch scheduling across multiple production units. *Journal of Engineering Management and Systems Engineering*, 3(1), 1-20. <https://doi.org/10.56578/jemse030101>
- [16] Brännlund, U., et al. (1998). Railway timetabling using Lagrangian relaxation. *Transportation science*, 32(4), 358-369. <https://doi.org/10.1287/trsc.32.4.358>
- [17] Caprara, A., et al. (2006). A Lagrangian heuristic algorithm for a real-world train timetabling problem. *Discrete applied mathematics*, 154(5), 738-753. <https://doi.org/10.1016/j.dam.2005.05.026>
- [18] Zhou, W. and H. Teng. (2016). Simultaneous passenger train routing and timetabling using an efficient train-based Lagrangian relaxation decomposition. *Transportation Research Part B: Methodological*, 94, 409-439. <https://doi.org/10.1016/j.trb.2016.10.010>
- [19] Zhou, W., et al. (2017). Multi-periodic train timetabling using a period-type-based Lagrangian

- relaxation decomposition. *Transportation Research Part B: Methodological*, 105, 144-173. <https://doi.org/10.1016/j.trb.2017.08.005>
- [20] Cacchiani, V., A. Caprara, and P. Toth. (2008). A column generation approach to train timetabling on a corridor. *4or*, 6, 125-142. <https://doi.org/10.1007/s10288-007-0037-5>
- [21] Pan, H., L. Yang, and Z. Liang. (2023). Demand-oriented integration optimization of train timetabling and rolling stock circulation planning with flexible train compositions: A column-generation-based approach. *European Journal of Operational Research*, 305(1), 184-206. <https://doi.org/10.1016/j.ejor.2022.05.039>
- [22] Cai, X. and C. Goh. (1994). A fast heuristic for the train scheduling problem. *Computers & Operations Research*, 21(5), 499-510. [https://doi.org/10.1016/0305-0548\(94\)90099-X](https://doi.org/10.1016/0305-0548(94)90099-X)
- [23] Neamah, N.M., B.A. Kalaf, and W. Mansoor. (2023). Solving Tri-criteria: Total Completion Time, Total Earliness, and Maximum Tardiness Using Exact and Heuristic Methods on Single-Machine Scheduling Problems. *Mathematical modelling of engineering problems*, 11(4), 987-995. <https://doi.org/10.18280/mmep.110415>
- [24] Lee, Y. and C.-Y. Chen. (2009). A heuristic for the train pathing and timetabling problem. *Transportation Research Part B: Methodological*, 43(8-9), 837-851. <https://doi.org/10.1016/j.trb.2009.01.009>
- [25] Karoonsoontawong, A. and A. Taptana. (2017). Branch-and-bound-based local search heuristics for train timetabling on single-track railway network. *Networks and Spatial Economics*, 17, 1-39. <https://doi.org/10.1007/s11067-015-9316-4>
- [26] Puška, A., et al. (2024). Optimising AGV routing in container terminals: Nearest neighbor vs. Tabu search. *Mechatronics and Intelligent Transportation Systems (MITS)*, 3(4), 203-211. <https://doi.org/10.56578/mits030401>
- [27] Zhou, W., et al. (2011). Method of integrated optimization of train operation plan and diagram for network of dedicated passenger lines. *Journal of the China Railway Society*, 2.
- [28] Kaspi, M. and T. Raviv. (2013). Service-oriented line planning and timetabling for passenger trains. *Transportation Science*, 47(3), 295-311. <https://doi.org/10.1287/trsc.1120.0424>
- [29] Yang, L., et al. (2016). Collaborative optimization for train scheduling and train stop planning on high-speed railways. *Omega*, 64, 57-76. <https://doi.org/10.1016/j.omega.2015.11.003>
- [30] Yue, Y., et al. (2016). Optimizing train stopping patterns and schedules for high-speed passenger rail corridors. *Transportation Research Part C: Emerging Technologies*, 63, 126-146. <https://doi.org/10.1016/j.trc.2015.12.007>
- [31] Niu, H., X. Zhou, and R. Gao. (2015). Train scheduling for minimizing passenger waiting time with time-dependent demand and skip-stop patterns: Nonlinear integer programming models with linear constraints. *Transportation Research Part B: Methodological*, 76, 117-135. <https://doi.org/10.1016/j.trb.2015.03.004>
- [32] Jiang, F., V. Cacchiani, and P. Toth. (2017). Train timetabling by skip-stop planning in highly congested lines. *Transportation Research Part B: Methodological*, 104, 149-174. <https://doi.org/10.1016/j.trb.2017.06.018>